Jet and bulk observables within a partonic transport approach

Florian Senzel
with J. Uphoff, O. Fochler, C. Wesp, Z. Xu and C. Greiner
based on Phys.Rev.Lett. 114 (2015) 112301

GOETHE UNIVERSITÄT FRANKFURT AM MAIN

Transport meeting, 29.04.2015

H-QM Helmholtz Research School Quark Matter Studies

HGS-HIRe for FAIR Helmholtz Graduate School for Hadron and Ion Research

Outline

1. Motivation
2. The partonic transport model BAMPS
3. Recent results about the...
   - ... nuclear modification factor R_{AA}
   - ... elliptic flow v_2 and bulk properties
   - ... energy loss of reconstructed jets

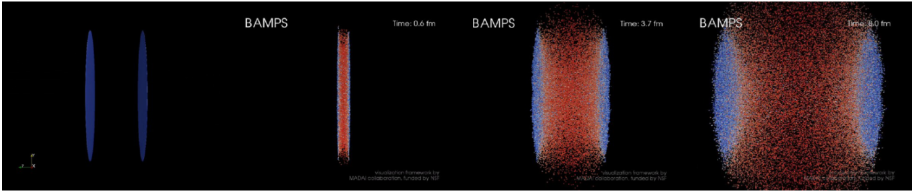

Visualization by Jan Uphoff
Visualization framework courtesy MADAI collaboration
funded by the NSF under grant NSF-PHY-09-41373

Tools for probing QCD matter: Ultra-relativistic heavy-ion collisions

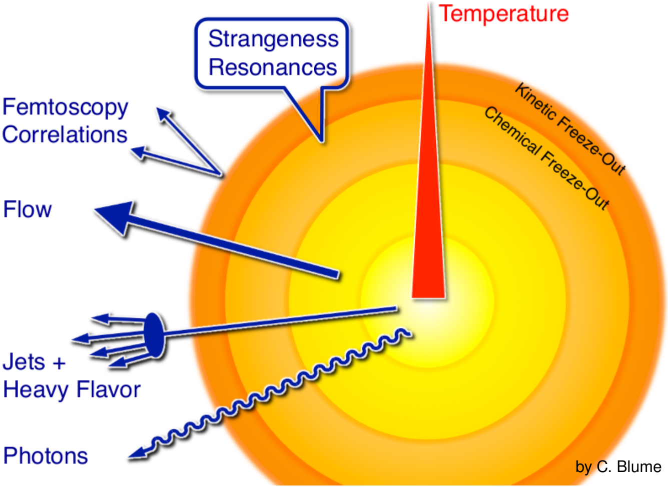

Collectivity of the bulk regime: Elliptic flow v_2

Fourier decomposition of particle spectra

$$\frac{d^3N}{p_t dp_t dy d\phi}(p_t, y, \phi) = \frac{1}{2\pi}\frac{d^2N}{p_t dp_t dy}\left[1 + 2v_2(p_t, y)\cos(2\phi) + \ldots\right]$$

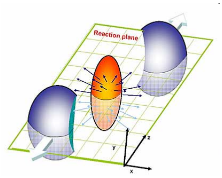

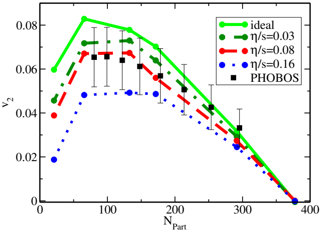

by Romatschke, Phys.Rev.Lett. 99, (2007)

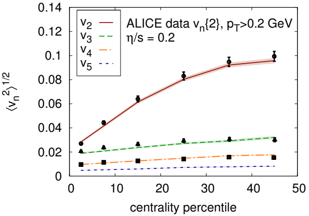

by Gale et al., Phys.Rev.Lett. 110 (2013)

State-of-the-art

✓ Well described by relativistic (viscous) hydrodynamics

Jet quenching: Nuclear modification factor R_{AA}

Suppression of inclusive particle spectra

$$R_{AA} = \frac{d^2N_{AA}/dp_t dy}{N_{bin}\, d^2N_{pp}/dp_t dy}$$

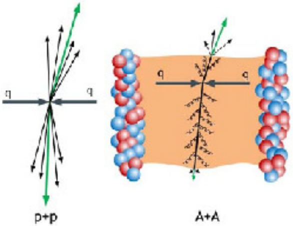

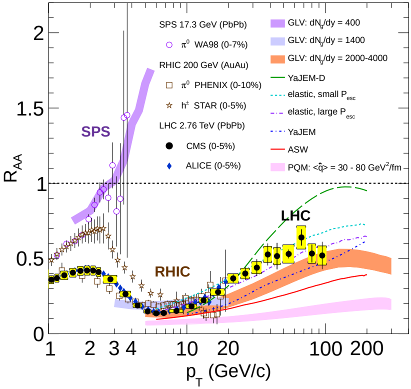

by CMS Collaboration, Eur. Phys. J. C (2012)

State-of-the-art

✓ Well described by perturbative quantum chromodynamics

Our question:

Can perturbative QCD interactions explain in a common framework

both the high p_t and the bulk medium regime

and thereby give microscopical insight into the QGP?

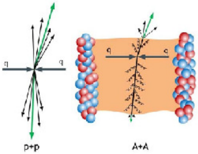

pQCD? $\longleftrightarrow$

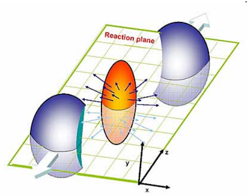

The partonic transport model BAMPS

BAMPS $\widehat{=}$ Boltzmann Approach to Multi-Parton Scattering[1]

Numerical solver for the (3+1)D Boltzmann transport equation for partons on the mass-shell:

$$\frac{\partial f}{\partial t} + \frac{\mathbf{p}}{E}\frac{\partial f}{\partial \mathbf{r}} = C_{2\rightarrow 2} + C_{2\leftrightarrow 3}$$

- Massless particles (gluons & quarks)
- Discretized space ΔV and time Δt:

$$P_{2\rightarrow 2} = v_{rel}\sigma_{2\rightarrow 2}\frac{\Delta t}{\Delta V} \qquad P_{2\rightarrow 3} = v_{rel}\sigma_{2\rightarrow 3}\frac{\Delta t}{\Delta V}$$

$$P_{3\rightarrow 2} = \frac{I_{3\rightarrow 2}}{8E_1E_2E_3}v_{rel}\frac{\Delta t}{\Delta V^2}$$

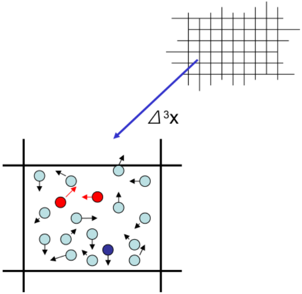

- Test-particles ansatz N_{test}

[1] Xu and Greiner, Phys.Rev.C71 (2005); Xu and Greiner, Phys.Rev.C76 (2007)

Implemented processes - elastic collisions

Screened matrix elements

$$\left|\overline{\mathcal{M}}_{X\to Y}\right|^2 = C_{X\to Y}\, 64\pi^2\alpha_s^2 \frac{s^2}{[t - m_D^2(\alpha_s)]^2}$$

$$\text{with } m_D^2(\alpha_s) = d_G \pi\alpha_s \int \frac{d^3p}{(2\pi)^3}\frac{1}{p}\left(N_c f_g + N_f f_q\right)$$

LO pQCD cross-sections

$$\begin{array}{lllll}
g\,g & \to & g\,g & & \\
g\,g & \to & q\,\bar{q} & & \\
q\,\bar{q} & \to & g\,g & \text{and} & q\,\bar{q} \to q'\,\bar{q}' \\
q\,g & \to & q\,g & \text{and} & \bar{q}\,g \to \bar{q}\,g \\
q\,\bar{q} & \to & q\,\bar{q} & & \\
q\,q & \to & q\,q & \text{and} & \bar{q}\,\bar{q} \to \bar{q}\,\bar{q} \\
q\,q' & \to & q\,q' & \text{and} & q\,\bar{q}' \to q\,\bar{q}'
\end{array}$$

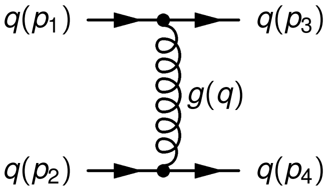

Uphoff, Fochler, Xu, Greiner: Phys.Rev.C84 (2011)

Implemented processes - radiative processes

Improved Gunion-Bertsch ME

$$\left|\overline{\mathcal{M}}_{X\rightarrow Y+g}\right|^2 = \left|\overline{\mathcal{M}}_{X\rightarrow Y}\right|^2 48\pi\alpha_s \left(1-\bar{x}\right)^2 \times \left[\frac{\mathbf{k}_\perp}{k_\perp^2} + \frac{\mathbf{q}_\perp - \mathbf{k}_\perp}{(\mathbf{q}_\perp - \mathbf{k}_\perp)^2 + m_D^2\left(\alpha_s\right)}\right]^2$$

with $\bar{x} = k_\perp e^{|y|}/\sqrt{s}$

$2 \rightarrow 3$ processes

$$\begin{array}{lllllll} g\,g & \rightarrow & g\,g\,g & & & & \\ q\,g & \rightarrow & q\,g\,g & \text{and} & \bar{q}\,g & \rightarrow & \bar{q}\,g\,g \\ q\,\bar{q} & \rightarrow & q\,\bar{q}\,g & & & & \\ q\,q & \rightarrow & q\,q\,g & \text{and} & \bar{q}\,\bar{q} & \rightarrow & \bar{q}\,\bar{q}\,g \\ q\,q' & \rightarrow & q\,q'\,g & \text{and} & \bar{q}\,\bar{q}' & \rightarrow & \bar{q}\,\bar{q}'\,g \end{array}$$

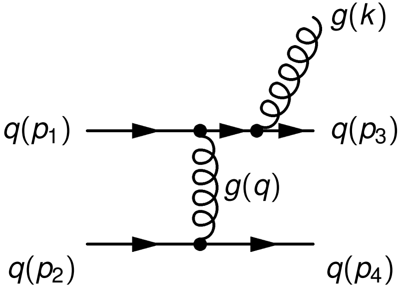

Gunion, Bertsch: Phys.Rev.D25 (1982)
Fochler, Uphoff, Xu, Greiner: Phys.Rev.D88 (2013)

Improved Gunion-Bertsch matrix element

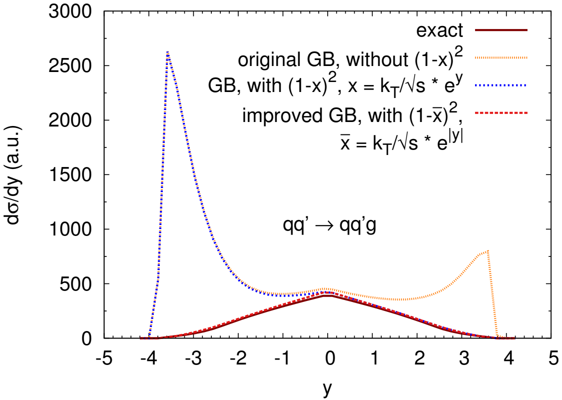

- Infrared screening for both GB and exact: $\theta\,(\text{cut}) = \theta\,\left(p_i p_j - \lambda\right)$.
- Integration both in GB coordinates and in standard phase space with numeric δ-functions.

Running coupling evaluated at the microscopic scale

$2 \to 2$ processes

$$\alpha_s \to \alpha_s(Q^2)$$

with $Q^2 \in \{s, t, u\}$

$2 \to 3$ processes

$$\alpha_s \to \alpha_s(Q^2)$$

with $Q^2 \in \{k_t, q_t\}$

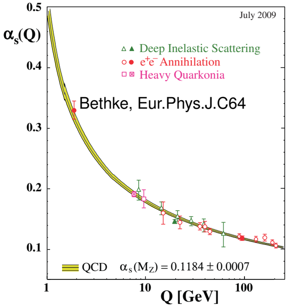

Remark

Due to universality arguments [1], the running coupling can be limited by $\alpha_{s;\max} = 1.0$.

[1] Y. Dokshitzer, Nucl.Phys. A711, 11 (2002)

Effective modeling of the LPM effect

Issue

Coherence effects within a semi-classical approach are not trivial.

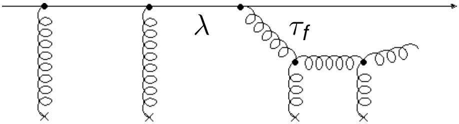

Effective method

Parent parton is not allowed to scatter before emitted gluon is formed:

$$|\mathcal{M}_{2\to3}|^2 \to |\mathcal{M}_{2\to3}|^2 \, \Theta\left(\lambda - X_{\mathrm{LPM}}\, \tau_f\right)$$

$X_{\mathrm{LPM}} = 0$	No LPM suppression
$X_{\mathrm{LPM}} = 1$	Only independent scatterings (forbids too many emissions)
$X_{\mathrm{LPM}} \in (0;1)$	Allows effectively some collinear gluons

Resulting differential $2 \to 3$ cross-sections

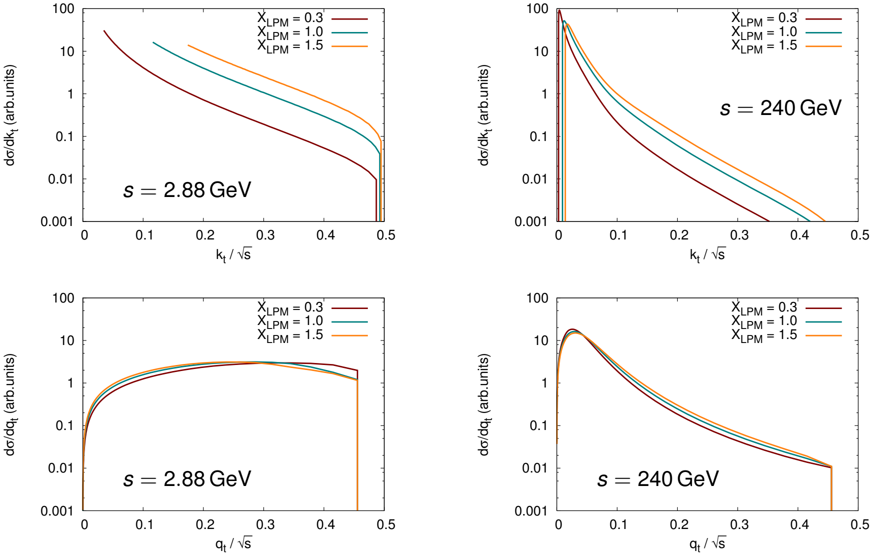

Dependence of the differential energy loss on X_{LPM}

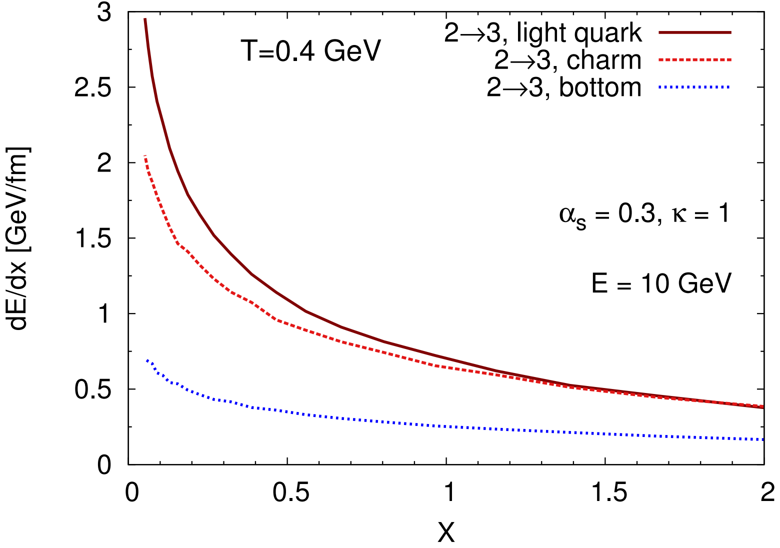

Differential energy loss in a static medium

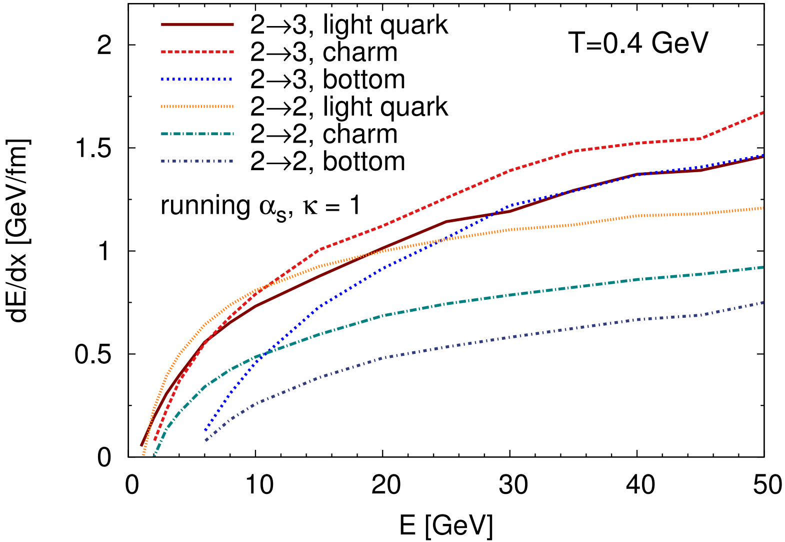

From partons to hadronic observables

"High p_t" observables

- Folding with fragmentation functions $D_i^h\left(z, Q^2\right)$,

$$\frac{\mathrm{d}^2 N^h}{\mathrm{d}p_t \mathrm{d}y}\left(p_t^h\right) = \sum_i \int_{z_{min}}^1 \mathrm{d}z \frac{\mathrm{d}^2 N^i}{\mathrm{d}p_t \mathrm{d}y}\left(\frac{p_t^h}{z}\right) D_i^h\left(z, Q^2\right) \text{ with } z = \frac{p_t^h}{p_t^i}$$

partons i

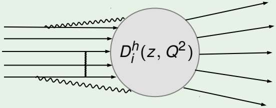

hadrons h

Fragmentation functions by e.g. Albino, Kniehl, Kramer: Nucl.Phys.B803(2008)

"Low p_t" observables

- Microscopic hadronization processes are unknown.
- Assuming parton-hadron duality, the integrated flow is not modified during hadronization.

Nuclear modification factor R_{AA} of central HI-collisions

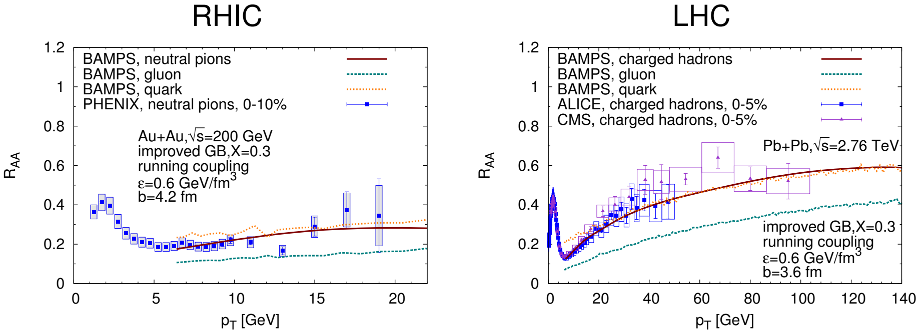

- PYTHIA initial conditions distributed by Glauber.
- After fixing the LPM parameter $X_{\mathrm{LPM}} = 0.3$ by comparing to RHIC data, BAMPS describes the R_{AA} also at LHC.
- Suppression caused by the interplay between the improved GB matrix element and the microscopic running coupling.

R_{AA} of peripheral HI-collisions

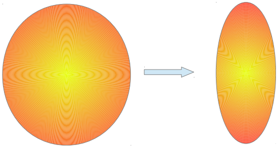

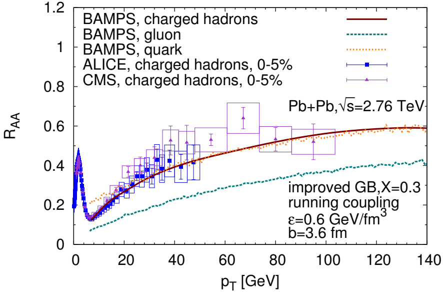

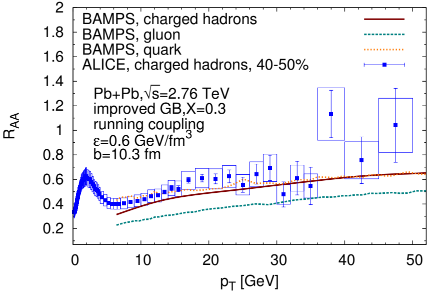

R_{AA} of central HI collisions for different hadron species

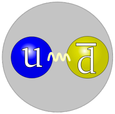

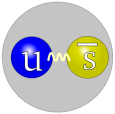

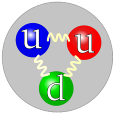

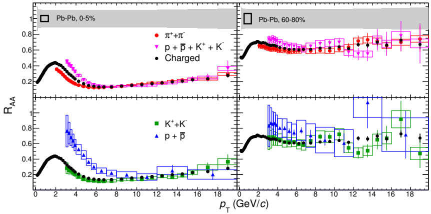

ALICE Collaboration, arXiv:1401.1250

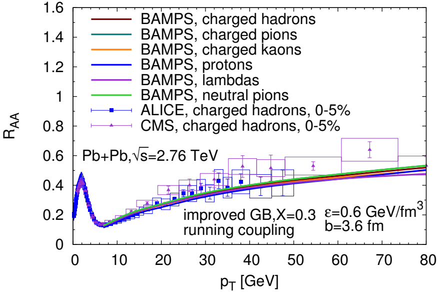

"Elliptic flow" $v_2\,(p_t)$ at high p_t

$$v_2 = \left\langle \frac{p_x^2 - p_y^2}{p_t^2} \right\rangle$$

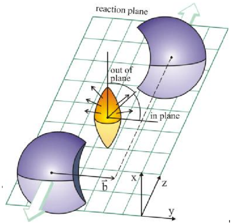

by B.Betz

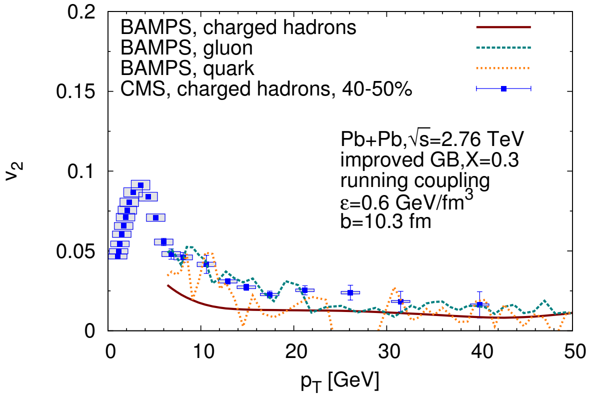

$v_2(p_t > 10\,\text{GeV})$ similar to other pQCD approaches (Betz, Gyulassy: JHEP 1408 (2014) 090).

Integrated elliptic flow $v_2\,(N_{\rm part})$

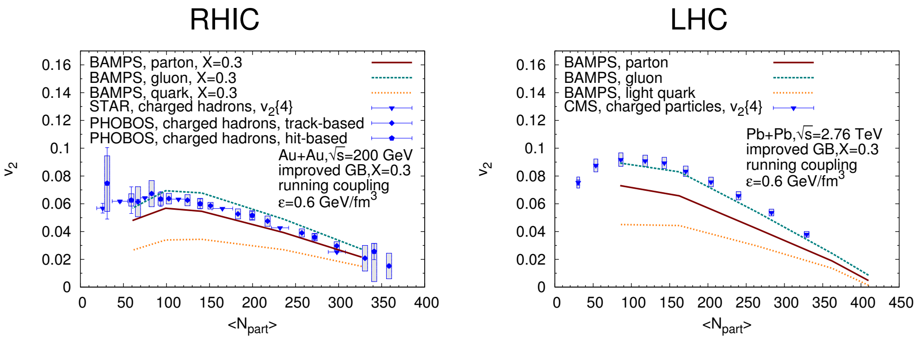

Same setup with LPM parameter $X_{\rm LPM} = 0.3$ leads to a sizable elliptic flow built up in the partonic phase.

Attention

No hadronization for bulk $\Rightarrow$ No hadronic after-burner $\Rightarrow$ Missing 10-20%?!

Momentum isotropy of the central region

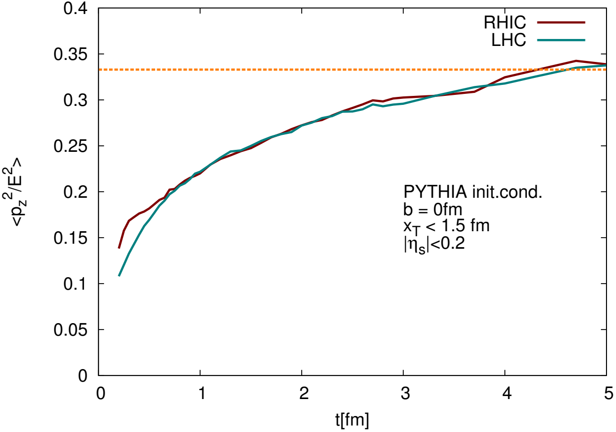

Thermalization

pQCD interactions lead to a thermalization time $\tau \approx 1\,\text{fm} - 2\,\text{fm}$.

Macroscopic quantities from microscopic interactions

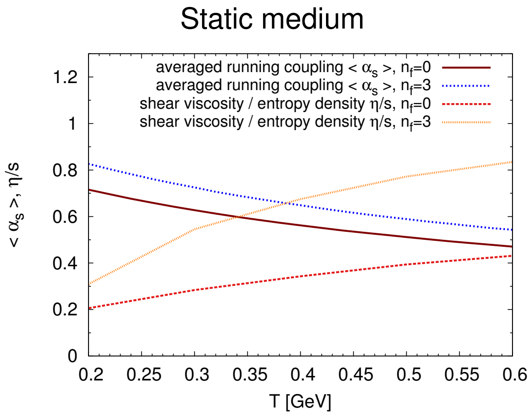

Shear viscosity ratio η/s

- Reason for large flow: small shear viscosity over entropy ratio
- Calculated with Green-Kubo formalism
- Recent viscous hydro: $\eta/s = 0.2$

Running coupling $\alpha_s(T)$

- Temperature dependent coupling by microscopically evaluated interactions.

Closer look on the distribution of α_s in a static medium

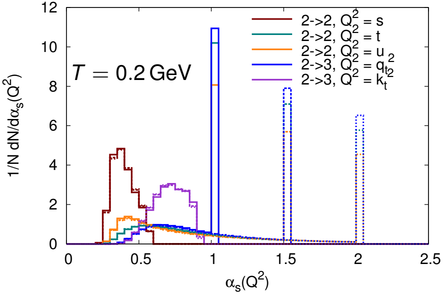

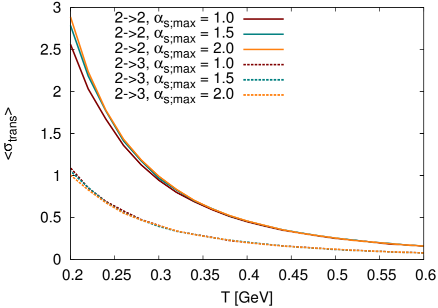

- Distributions of $\alpha_s(Q^2)$ are broad and have peaks at $\alpha_{s;\max}$.
- However, due to small momentum transfers the transport cross sections are insensitive to $\alpha_{s;\max}$.

Elliptic flow v_2 for different $\alpha_{s;\max}$ values

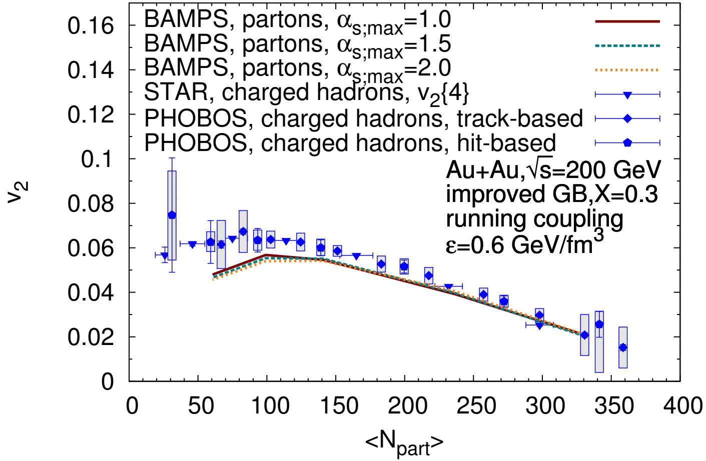

Reconstructed jets in heavy-ion collisions

⟶

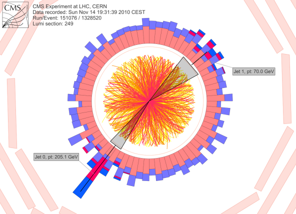

⟶

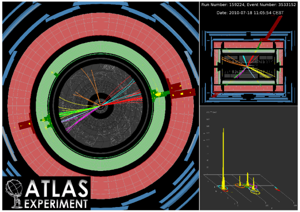

Momentum imbalance A_J of reconstructed di-jets

Definition

$$A_J = \frac{p_{t;Leading\ Jet} - p_{t;Subleading\ Jet}}{p_{t;Leading\ Jet} + p_{t;Subleading\ Jet}}$$

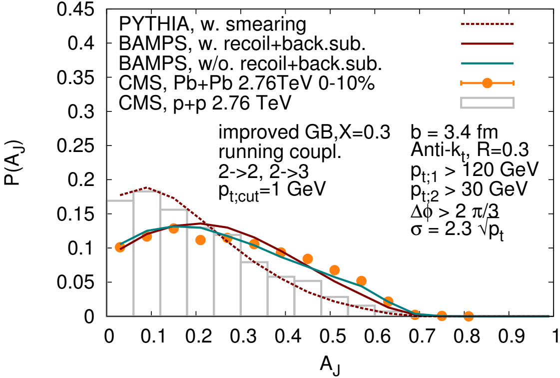

FS, Fochler, Uphoff, Xu, Greiner: arXiv:1309.1657

Jet R_{AA} in comparison with jet R_{CP} data

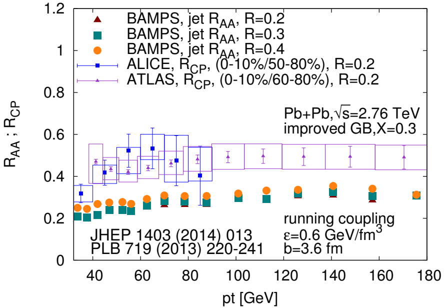

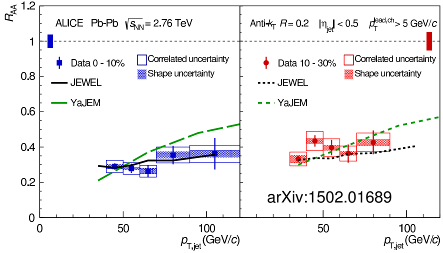

Attention: Preliminary!

Quantitative comparison study with jet R_{AA} data is in progress.

Conclusions

- Partonic transport provides means for..
  - exploring dynamics of the QGP evolution based on pQCD processes.
  - exploring different observables within a common framework.
- Realistic suppression of jets both at RHIC and LHC.
- Sizable collective flow within the medium by microscopic pQCD cross sections.

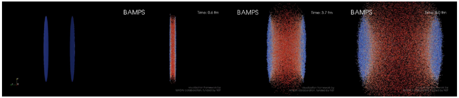

Future plans:

- How does a revisited modeling of the LPM effect change the energy loss and its path-length dependence?
- More systematic comparison with data!
  (jet+γ-, jet+h-, h+h-correlations, future collider energies. . .)

Outlook - R_{AA} of LHC Run 2

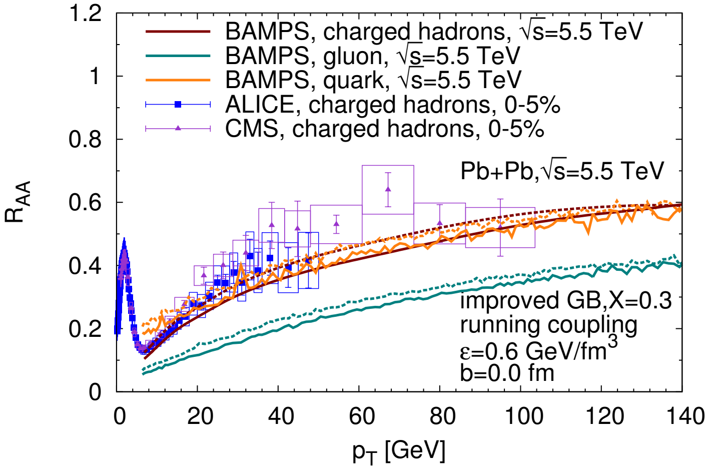

Conclusions

- Partonic transport provides means for..
  - exploring dynamics of the QGP evolution based on pQCD processes.
  - exploring different observables within a common framework.
- Realistic suppression of jets both at RHIC and LHC.
- Sizable collective flow within the medium by microscopic pQCD cross sections.

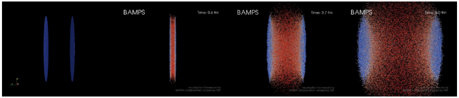

Future plans:

- How does a revisited modeling of the LPM effect change the energy loss and its path-length dependence?
- More systematic comparison with data!
  (jet+γ-, jet+h-, h+h-correlations, future collider energies. . .)

Backup slides

Closer look on the role of fragmentation

Probability for hadron h with p_t^h out of parton i with $p_t^i = p_t^h / z$

$$P^{i\to h}\left(z, p_t^h\right) = \frac{1}{\frac{d^2N^h}{dp_t dy}\left(p_t^h\right)} \frac{d^2N^i}{dp_t dy}\left(\frac{p_t^h}{z}\right) D_i^h\left(z, Q^2\right)$$

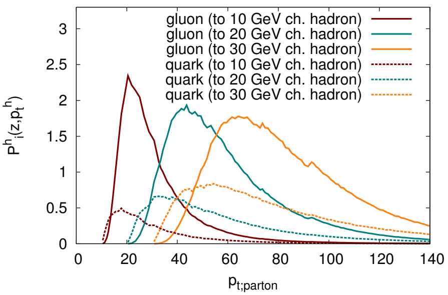

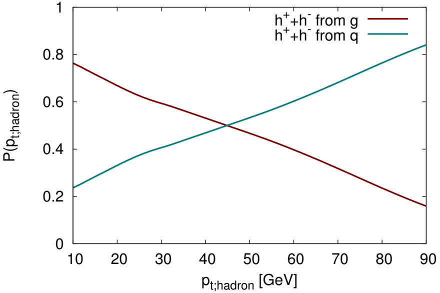

Example: R_{AA} for hadrons with $p_t^h = 30\,\text{GeV}$

Hadrons with $p_t^h = 30\,\text{GeV}$ stem...

... mainly from $\approx 60\,\text{GeV}$ gluon and $\approx 45\,\text{GeV}$ quark.

... $\approx 60\,\%$ from gluons and $\approx 40\,\%$ from quarks. 6

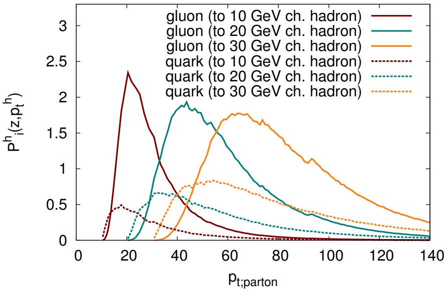

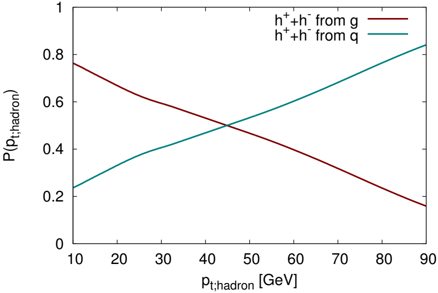

Example: R_{AA} for hadrons with $p_t^h = 30\,\text{GeV}$

Hadrons with $p_t^h = 30\,\text{GeV}$ stem...

... mainly from $\approx 60\,\text{GeV}$ gluon and $\approx 45\,\text{GeV}$ quark.

... $\approx 60\,\%$ from gluons and $\approx 40\,\%$ from quarks. 6

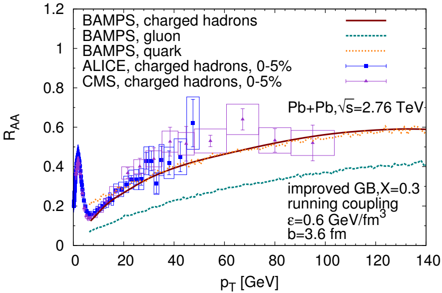

$$R^h_{AA}(30\,\text{GeV}) = 0.4\,R^g_{AA}(60\,\text{GeV}) + 0.6\,R^q_{AA}(45\,\text{GeV}) \approx 0.3$$

Example: Shower event with first 100 recoil partons

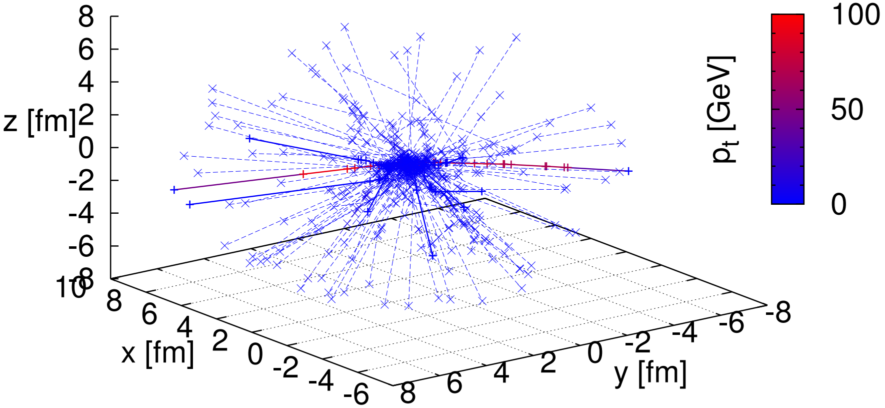

Dependence of heavy-ion observables on X_{LPM}

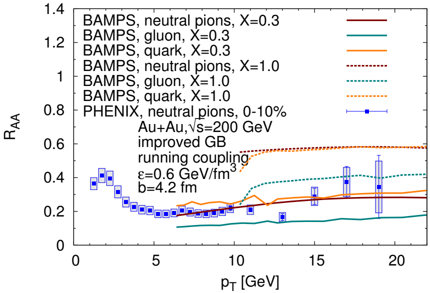

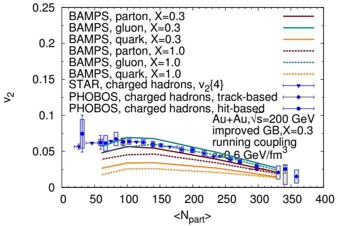

Figure: Elliptic flow v_2 of gluons, light quarks, and both together (light partons) within $|\eta| < 1.0$ as a function of the number of participants N_{part} at RHIC for a running coupling and two different LPM parameter $X \in 0.3, 1.0$. As a comparison we show experimental data by STAR and PHOBOS for charged hadrons within $|\eta| < 0.5$ and $|\eta| < 1.0$.